COUPLING OF HEAT DRIVEN MODES IN THE RIJKE TUBE

Alessandra Bigongiari and Maria Heckl

Deparment of Mathematics, Keele University, Staffordshire ST5 5GB, UK

e-mail: a.bigongiari@keele.ac.uk

A new model describing the coupling of heat driven modes in a Rijke tube is presented. The heat source is assumed to be compact and to have a linear heat release characteristic with a time lag. The equations for the eigenmodes are solved using a different number of Green function modes and the stability behavior of the system is analyzed. The Green function, which we derive for this configuration, is a superposition of modes with eigenfreqencies ω_n and corresponding amplitudes. We use a Green function approach to derive the characteristic equation for the complex eigenfrequencies Ω_m of the heat driven modes. This equation reveals which parameters are essential for the mode coupling.

1.   Introduction

An unsteady heat source within a duct can be a source of large amplitude oscillations of the acoustic field. These oscillations are the result of the superposition of the heat driven modes of the tube, which depend on the tube parameters and the heat source characteristics. In this paper we wish to take a step forward in the understanding of the nonlinear interaction between modes, and how this affects the stability of the system.

We introduce a model for the coupling of the heat driven modes in the Rijke tube, using a Green function approach. The Rijke tube is a simplified model of a burner as shown in Fig. 1.
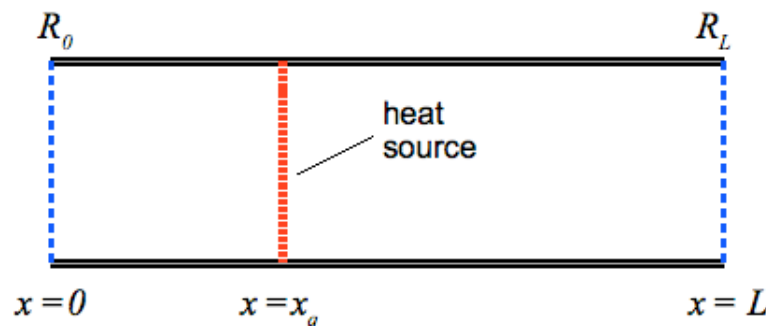

Figure 1: Rijke tube with a point source at $x = x_q$.

We assume the acoustic field in the tube to be one-dimensional . The tube has open ends, and these are modeled by the reflection coefficient of Levine and Schwinger[1]

$$R_0 = R_L = -\frac{1 - \left[\frac{1}{4}\left(\frac{\omega a}{c}\right)^2 - i\frac{\omega a}{c}\delta\right]}{1 + \left[\frac{1}{4}\left(\frac{\omega a}{c}\right)^2 - i\frac{\omega a}{c}\delta\right]} \tag{1}$$

for both ends, where a is the diameter of the tube, c is the speed of sound and $\delta = 0.6133$ represents the end correction. The heat source is compact and located at $x = x_q$, so that the heat release rate can be written as

$$q(x, t) = q(t)\delta(x - x_q) \tag{2}$$

$q(x, t)$ is a local heat release rate (i.e. the heat release rate per unit mass) and has units of power per unit mass.

2. The Green function approach

A Green function approach can be used to calculate the acoustic velocity in the duct. The Green function is the velocity potential created in the tube at position x and time t by an impulsive point source located at x' and firing at time t'. It is obtained as the solution of the governing equation

$$\frac{1}{c^2}\frac{\partial^2 G}{\partial t^2} - \frac{\partial G}{\partial x^2} = \delta(x - x')\delta(t - t') \tag{3}$$

with the boundary conditions described by the reflection coefficients R_0 and R_L. It is a superposition of acoustic modes of amplitudes g_n and frequencies ω_n

$$G(x, x', t, t') = H(t - t')\sum_{n=0}^{\infty} \Im\left[g_n(x, x')e^{-i\omega_n(t - t')}\right]. \tag{4}$$

The modal amplitudes and frequencies can be calculated for different characteristics of the duct, such as a jump in the cross-sectional area[2], a blockage[3], or a temperature gradient[4]. For the case of a simple Rijke tube, with uniform temperature and constant cross-sectional area, ω_n is given by the characteristic equation $F(\omega) = 0$ with

$$F(\omega) = i2\frac{\omega}{c}\left(1 - R_L R_0 e^{i2L\frac{\omega}{c}}\right) \tag{5}$$

The modal amplitudes g_n are given by

$$g_n(x, x', \omega_n) = -\frac{ic^2 e^{-i2L\frac{\omega_n}{c}}}{4\omega_n R_0 R_L}\left(R_0 e^{i\frac{\omega_n}{c}x} + e^{-i\frac{\omega_n}{c}x}\right)\left(e^{i\frac{\omega_n}{c}x'} + e^{-i\frac{\omega_n}{c}(x'-2L)}R_L\right). \tag{6}$$

Many mathematical steps are required to obtain results (5) and (6). These are not shown here; details about the derivation method can be found in Heckl[5]. The velocity potential, denoted here by $\Phi(x, t)$, is governed by the acoustic analogy equation

$$\frac{1}{c^2}\frac{\partial^2 \Phi}{\partial t^2} - \frac{\partial \Phi}{\partial x^2} = -\frac{\gamma - 1}{c^2}q(t) \tag{7}$$

An integral equation can be derived from Eq. (3) and Eq. (7) which gives the time history of the acoustic velocity as

$$u(x_q,t)=\frac{\partial \Phi}{\partial x}\Big|_{x=x_q}=-\frac{\gamma-1}{c^2}\int_{t'=0}^{t}\frac{\partial G(x,x',t,t')}{\partial x}\Big|_{\substack{x=x_q\\x'=x_q}}q(t')dt'-\frac{\varphi_0}{c^2}\frac{\partial G}{\partial x \partial t'}\Big|_{\substack{t'=0\\x'=x_q}}+\frac{\varphi_0'}{c^2}\frac{\partial G}{\partial x}\Big|_{\substack{t'=0\\x'=x_q}} \quad (8)$$

The integral term represents the response to "forcing" by the heat release rate. The last two terms are due to the initial conditions

$$\frac{\partial \Phi(x,t)}{\partial t}\Big|_{t=0}=\varphi_0'\delta(x-x_q) \quad \text{and} \quad \Phi(x,t)\big|_{t=0}=\varphi_0\delta(x-x_q) \ . \quad (9)$$

These represent an initial disturbance at the heat source, whose strength is given by the constants φ_0 and φ_0'. For details of the derivation see Heckl and Howe[2].

3.   Frequency domain calculation of the acoustic velocity

3.1   General method

We now investigate the coupling of the natural tube modes and how this affects the stability of the system. To this aim we represent the acoustic velocity as a superposition of heat driven modes, with complex modal amplitudes u_m and heat driven frequencies Ω_m.

$$u(t)=\sum_{m=1}^{\infty}\left[u_m e^{-i\Omega_m t}+u_m^* e^{i\Omega_m^* t}\right]; \quad (10)$$

the superscript [*] denotes the complex conjugate.

An acoustic mode n in the Rijke tube now has two distinctly different frequencies associated with it: ω_n and Ω_n. ω_n is the resonance frequency without fluctuating heat source and Ω_n is that with fluctuating heat source. ω_n has an imaginary part that is always negative (due to dumping in the system), whereas Ω_n can have negative or positive imaginary part; a positive imaginary part indicates that mode n is unstable due to thermoacoustic feedback.

We will now assume a linear heat release law:

$$q(t)=K\cdot u(t-\tau) \quad (11)$$

where K is a coupling constant and τ is a time delay. Substituting Eqs. (4), (10) and (11) into Eq. (8) we get

$$\sum_{m=1}^{\infty}\left[u_m e^{-i\Omega_m t}+u_m^* e^{i\Omega_m^* t}\right]=\frac{BK}{2}\int_{t'=0}^{t}\sum_{n=1}^{\infty}\left[G_n e^{-i\omega_n(t-t')}+G_n^* e^{i\omega_n^*(t-t')}\right]\sum_{m=1}^{\infty}\left[u_m e^{-i\Omega_m(t'-\tau)}+u_m^* e^{i\Omega_m^*(t'-\tau)}\right]dt'$$
$$+\frac{1}{2c^2}\sum_{n=1}^{\infty}\left[(\varphi_0'-\varphi_0 i\omega_n)G_n e^{-i\omega_n t}+(\varphi_0'+\varphi_0 i\omega_n^*)G_n^* e^{i\omega_n^* t}\right] \quad (12)$$

where the abbreviation

$$B=-\frac{(\gamma-1)}{c^2} \quad (13)$$

has been used , and G_n denotes the Green's function amplitude in terms of the *velocity,*

$$G_n = i \frac{\partial g_n}{\partial x} . \tag{14}$$

From Eq. (12) it is possible to derive equations for the complex amplitudes u_m and frequencies Ω_m. Details of the derivation can be found in Heckl and Howe[2]. Here we just summarize the results. The equation for Ω_m is non-linear and has the form

$$\sum_{n=1}^{\infty} \frac{G_n e^{i\Omega_m \tau}}{i(\omega_n - \Omega_m)} - \frac{G_n^* e^{i\Omega_m \tau}}{i(\omega_n^* + \Omega_m)} = \frac{2}{K B} \quad m=1,2,3... \tag{15}$$

This is a *single* equation for Ω_m; the frequencies of other heat driven modes do not appear in it. This make it relatively easy to solve Eq. (15). The amplitudes u_m, and their complex conjugate u_m^* are given by the following set of linear equations,

$$\sum_{m=1}^{\infty} \frac{u_m e^{i\Omega_m \tau}}{i(\omega_n - \Omega_m)} + \frac{u_m^* e^{-i\Omega_m^* \tau}}{i(\omega_n + \Omega_m^*)} = \frac{\varphi' - i\omega \varphi_0}{K B c^2} \quad \text{and} \quad \sum_{m=1}^{\infty} \frac{u_m e^{i\Omega_m \tau}}{i(\omega_n^* + \Omega_m)} + \frac{u_m^* e^{-i\Omega_m^* \tau}}{i(\omega_n^* - \Omega_m^*)} = \frac{-\varphi' - i\omega^* \varphi_0}{K B c^2} \tag{16}$$

We observe that Eq. (15) give the frequency Ω_m of the heat driven mode m in terms of the frequencies $\omega_1, \omega_2, \omega_3, ...$ and amplitudes $G_1, G_2, G_3, ...$ of the Green's function. We also notice that the time delay τ is a parameter that affects both Ω_m and u_m.

3.2   Calculation of the eigenfrequencies of the heat driven modes

We consider a Rijke tube of length $L = 1m$, diameter $a = 0.093m$ and $c = 350$ *m/s* (corresponding to experimental parameters in Gopalakrishnan[6]). The heater power is K=$5 \cdot 10^5$ *W s* $m^{-1}kg^{-1}$, $\gamma = 1.4$ and the the time-lag τ is varied. The heat source position is $x_q = 0.3L$.
The frequencies ω_n of the Green's function are calculated by solving Eq. (5) numerically with the Newton-Raphson method. The results are shown in Table 1 for the first three modes. Also shown are the Green's function amplitudes G_n, which were calculated from Eq. (6) and Eq. (14).

Table 1. Values of ω_n ($Hz/2\pi$) and G_n (s^{-1}) for $L = 1m$, $a = 0.093m$ and $c = 350$ *m/s*, $x_q = 30cm = 0.3L$.

n	ω_n	G_n
1	$986 - i\, 2.61 \cdot 10^{-14}$	$-111 - i148$
2	$1970 - i1.021 \cdot 10^{-15}$	$-16.9 + i135$
3	$2940 - i\, 2.67 \cdot 10^{-14}$	$-52.8 + i18.9$

We now use the values in Table 1 to determine the properties of the heat driven modes. The frequencies Ω_m are calculated from Eq. (15), with the sum truncated at three different thresholds: one term only ($n=1$), first two terms ($n=1, 2$) and first three terms ($n=1, 2, 3$). The results for Ω_1 and Ω_2 are shown in Table 2. The values of the time-lag τ are listed in the first column. The subsequent three columns show Ω_1 and Ω_2 for the three truncation thresholds mentioned above.

Table 2. Values of Ω_m ($Hz/2\pi$) as a function of ω_n and τ , $x_q = 30cm = 0.3L$.

τ	ω_1	$\omega_1 + \omega_2$	$\omega_1 + \omega_2 + \omega_3$
$\tau = 0.2\ ms = 0.03T_1$	$\Omega_1 = 1100 + i23.3$	$\Omega_1 = 1120 + i32.1$ $\Omega_2 = 1830 - i33.2$	$\Omega_1 = 1130 + i3.43$ $\Omega_2 = 1820 - i3.58$
$\tau = 1.8\ ms = 0.28T_1$	$\Omega_1 = 973 + i99.7$	$\Omega_1 = 962 + i96.2$ $\Omega_2 = 2070 + i35.4$	$\Omega_1 = 959 + i95.4$ $\Omega_2 = 2062 + i31.4$
$\tau = 3.4\ ms = 0.53T_1$	$\Omega_1 = 871 + i22.7$	$\Omega_1 = 881 + i13.1$ $\Omega_2 = 1840 + i26.6$	$\Omega_1 = 884 + i10.5$ $\Omega_2 = 1840 + i33.9$

$\tau = 5.0\ ms = 0.78 T_1$	$\Omega_1 = 1110 - i20.8$	$\Omega_1 = 808 - i188$ $\Omega_2 = 2040 + i47.9$	$\Omega_1 = 835 - i180$ $\Omega_2 = 2043 + i43.7$

The time-lags were chosen from a large range: from a very small fraction of T_1 (the period of the first mode, $T_1 = 2\pi/\omega_1 = 6.4 \cdot 10^{-3}\ s$) to nearly equal to T_1 .

We observe that the imaginary part of Ω_1 is negative for the first three τ values considered and positive for the last one. This means that the first mode, which is initially stable, becomes unstable for delays which are sufficiently large. Similarly, the second mode switches from unstable to stable. In general, from the Rayleigh criterion[7], we expect the stability of a mode to change for time-lags larger than half its period and smaller than one period. However as the real part of the heat driven frequency is also changing with the time-lag, the stability of each mode can not be determined by using the Rayleigh criterion. At the same time the heat driven frequency changes with the number of natural modes involved in the calculation. Therefore it is important to understand the role of the time-lag in the heat release and the interaction between its natural modes. In order to evaluate the effect of the resonant modes of the pipe, we investigate the transition from stable to unstable (and vice-versa) of the first two heat driven modes as a function of τ. In Table 3 we report the first two τ values for which we observe a change in the stability of each mode.

Table 3. Values of τ at the transition of each mode from stable to unstable (and vice-versa), $x_q = 30 cm = 0.3L$.

Ω	ω_1	$\omega_1 + \omega_2$	$\omega_1 + \omega_2 + \omega_3$
Ω_1	$\tau_1 = 3.70\ ms = 0.58 T_1$ $\tau_2 = 6.75\ ms = 1.05 T_1$	$\tau_1 = 3.55\ ms = 0.55 T_1$ $\tau_2 = 6.65\ ms = 1.04 T_1$	$\tau_1 = 3.55\ ms = 0.55 T_1$ $\tau_2 = 6.60\ ms = 1.03 T_1$
Ω_2	-	$\tau_1 = 1.65\ ms = 0.26 T_1$ $\tau_2 = 3.55\ ms = 0.55 T_1$	$\tau_1 = 1.65\ ms = 0.26 T_1$ $\tau_2 = 3.60\ ms = 0.56 T_1$

We observe that the transition value of τ tends to decrease when more natural modes of the pipe are taken into account and the difference is more evident for Ω_1.

### 3.3 Calculation of the amplitudes of the heat-driven modes

We will now use the results for Ω_1 and Ω_2 in Table 2 to find the modal amplitudes of the first two heat driven modes. In order to have enough equations to derive u_1 and u_2, we will write Eqs. (16) for $\omega_n = \omega_1$ and $\omega_n = \omega_2$. We obtain a system of four equations for the complex amplitudes which can be represented as a 4×4 matrix and solved for the unknown variables u_1, u_1^*, u_2, u_2^*. We will assume an infinitesimal perturbation for the initial values of the system, whose strength is expressed by the parameters $\varphi_0 = 10^{-9} m^3 s^{-1}$ and $\varphi_0' = 10^{-6} m^3 s^{-2}$. The results are given in Table 4 for different values of τ.

Table 4. Values of the modal amplitudes u_m (m/s) as a function of τ, $x_q = 30\ cm = 0.3L$.

$\tau = 0.2\ ms = 0.03 T_1$	$u_1 = (8.3 + i8.88) \cdot 10^{-10}$	$u_2 = (-1.54 - i0.678) \cdot 10^{-9}$
$\tau = 1.8\ ms = 0.28 T_1$	$u_1 = (4.56 + i4.89) \cdot 10^{-10}$	$u_2 = (-1.20 - i0.283) \cdot 10^{-9}$
$\tau = 3.4\ ms = 0.53 T_1$	$u_1 = (6.04 + i6.57) \cdot 10^{-10}$	$u_2 = (-1.33 - i0.449) \cdot 10^{-9}$
$\tau = 5.0\ ms = 0.78 T_1$	$u_1 = (5.21 + i4.66) \cdot 10^{-10}$	$u_2 = (-1.16 - i0.216) \cdot 10^{-9}$

3.4 The acoustic velocity

Substitution into Eq. (7) of he modal amplitudes in Table 4 and the corresponding heat-driven frequencies in Table 2, makes it possible to compute the acoustic velocity resulting from the contribution of the first two modes. The time evolution $u_q(t)$, for different values of the time lag is shown in Fig. 2, for the heater position $x_q = 30\ cm$, which is in the *upstream* half of the tube.
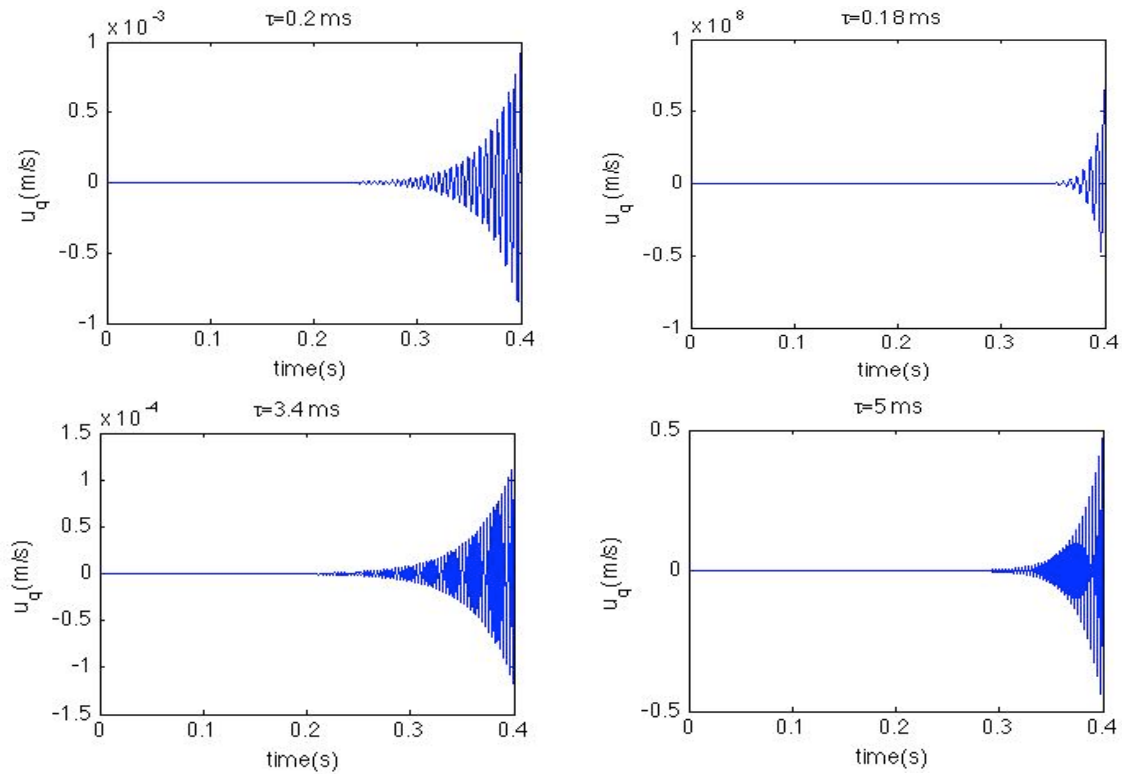
Figure 2 : Acoustic velocity at the heat source x_q=30cm =0.3L, for different values of τ.

The plots show that the model predicts instability for all τ values considered. We observe that for the smallest of the τ the first mode dominates, as we expected from the imaginary part sign of the respective frequencies. For larger time-lags, τ=5 ms the situation is reversed and the second mode dominates. We note that, as we used a linear heat release characteristic the instability does not saturate and that the amplitude of u_q grows without limit.

We will now investigate the stability of the system for a different heater position, x_q=70cm, which is in the downstream half of the Rijke tube, repeating the calculations in Sections 3.2 and 3.3. The results for the modal amplitudes and frequencies are summarized in Table 4 and the corresponding time evolution is shown in Fig. 3. We observe that the system is now stable for τ =1.8 ms, when both the first and the second mode are stable, while the instability grows for the remaining values of the time-lag.

Table 4. Values of Ω_m ($Hz/2\pi$) and u_m (m/s) as a function of τ, x_q=70 cm= 0.7L.

τ =0.2 ms =0.03T_1	Ω_1= 873− i9.76 Ω_2= 2050 + i49.3	u_1= (− 4.4 − i5.3)·10^{-10}	u_2=(8.5 + i5.5)·10^{-10}
τ =1.8 ms =0.28T_1	Ω_1= 988 − i161 Ω_2= 1830 − i40.6	u_1=(−9.5 − i6.9)·10^{-10}	u_2=(1.4 + i0.77)·10^{-9}
τ =3.4 ms =0.53T_1	Ω_1= 1080 + i53.1 Ω_2= 2030 + i55.8	u_1=(−6.3 − i4.5)·10^{-10}	u_2=(1.0+ i0.64)·10^{-9}
τ =5.0 ms =0.78T_1	Ω_1= 975 + i79.1 Ω_2= 1850 + i11.5	u_1=(−6.8 − i6.5)·10^{-10}	u_2=(1.0+ i0.75)·10^{-9}

Therefore the model predicts the growth/damping of the initial perturbation inside the Rijke tube as the combined result of the position of the heat source and its response to acoustic fluctuations. This is in agreement with our expectation as the instabilities grow when the oscillations of heat release and acoustic field are in phase, and this depends both on the time-lag and the heater position.
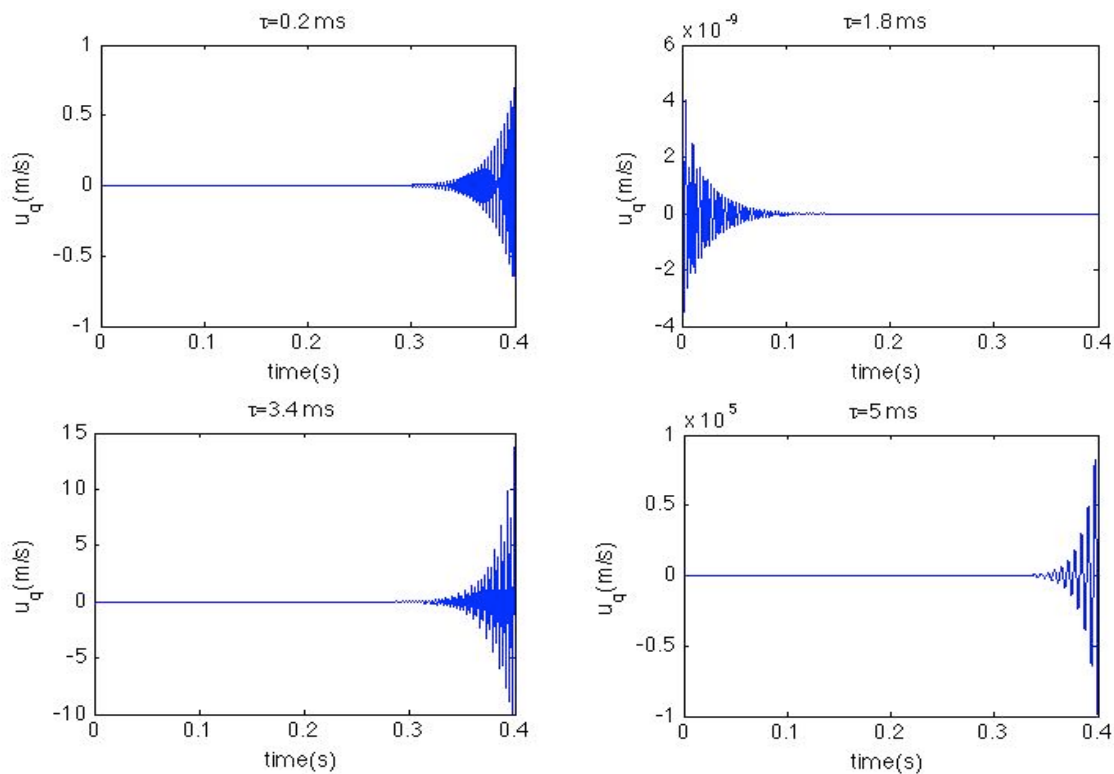
Figure 3 : Acoustic velocity at the heat source x_q=70 cm= 0.7L, for different values of τ.

4. Conclusions

We have presented a model which describes the coupling of the heat driven modes in a Rijke tube as a function of the tube parameters and the heat source characteristics.
An equation for the frequency of an individual heat-driven mode has been derived. This shows that the Green function modes, i.e. the resonant modes of the Rijke tube without unsteady heat release, and the time-lag, determine the coupling.
The stability of the system was analysed for two different source positions and different time-lags. The amplitudes of the heat driven modes were derived as a function of the initial conditions. Finally the time evolution of the acoustic velocity was obtained for different positions of the heat source.

The model is able to predict the linear stability of the system when a different number of resonant modes are taken into account. This is important as many precesses can be responsible for a selective response of the system to different acoustic modes. For example, it is known that the response of the heat source to different acoustic frequencies tend to damp some modes so that higher modes are not usually observed[7]. Losses and the presence of vorticity can also give a similar result. Therefore the model introduced in this paper represents a step forward in the understanding of the response of the system to perturbations and how the non-linear mode coupling affects the stability.

We plan to extend our analysis to pipes having different characteristics as a temperature distribution and a closed end.

ACKNOWLEDGEMENTS

REFERENCES

[1] Levine, H. and Schwinger, J. On the radiation of sound from an unflanged circular pipe, *Physical Review* **73**, 383-406, (1948).

[2] Heckl, M. and Howe, M. S. Stability analysis of the Rijke tube with a Green's function approach, *Journal of Sound and Vibration, 305, 672-688, (2007).*

[3] Heckl, M. and Kosztin, B. Analysis and control of an unstable mode in a combustor with tuneable end condition, *International journal of spray and combustion dynamics*, **5**(3), 243 – 272, (2013).

[4] Kosztin, B. Heckl, M., and Jakob Hermann Thermo-acoustic properties of a burner with axial temperature gradient: Theory and experiment, *International journal of spray and combustion dynamics*, **5**(1), 67 – 84, (2013).

[5] Heckl, M. Analytical model of nonlinear thermo-acoustic effects in a matrix burner, *Journal of Sound and Vibration,* **332**, 4021-4036, (2013).

[6] Gopalakrishnan, E. A. and Sujith, R. I. Influence of system parameters and external noise on hysteresis characteristics of a horizontal Rijke tube, *n3l - Int'l Summer School and Workshop on Non-Normal and Nonlinear Effects in Aero- and Thermoacoustics*, Munich, Germany, 18 – 21 June, (2013).

[7] Rayleigh, J. W. S. *The theory of sound*, Dover publications (1945, re-issue).